Available online at www.sciencedirect.com
SCIENCE DIRECT
Polymer 46 (2005) 5662–5672
polymer
www.elsevier.com/locate/polymer

New miscible blends composed of polysulfone and poly(1-vinylpyrrolidone-*co*-acrylonitrile) copolymers and their phase behavior

J.W. Kim, E.J. Moon, C.K. Kim*

School of Chemical Engineering and Materials Science, Chung-Ang University, 221 Huksuk-Dong, Dongjak-Gu, Seoul 156-756, South Korea

Received 6 October 2004; received in revised form 8 March 2005; accepted 25 March 2005

Abstract

The miscibility of polysulfone, PSf, blend with poly(1-vinylpyrrolidone), PVP, and that of PSf blend with poly(1-vinylpyrrolidone-*co*-acrylonitrile) copolymers, P(VP–AN), containing various amount of VP were explored. Even though PSf did not formed miscible blends with PVP when both components had high molecular weight, it formed miscible blend with PVP by decreasing molecular weight of PVP. PSf also formed homogeneous mixtures with P(VP–AN) containing AN from 2 to 16 wt%. These miscible blends underwent phase separation on heating caused by LCST-type (lower critical solution temperature-type) phase behavior. The phase separation temperature of miscible blends first increases with AN content, goes through a maximum centered at about 8 wt% AN. Interaction energies of binary pairs involved in blends were evaluated from the observed phase boundaries using the lattice–fluid theory. The decline of the contact angle between water and blend film by increasing P(VP–AN) content in blend indicated that the hydrophobic properties of PSf could be improved by blending with P(VP–AN) copolymers.

Keywords: Polysulfone; Poly(1-vinylpyrrolidone-*co*-acrylonitrile) copolymer; Miscible blends

1. Introduction

Blending of dissimilar polymers offers attractive opportunity for the development of novel materials with useful combination of properties [1–5]. Miscible polymer blends often exhibited improved properties in comparison with initial products but the immiscible blends often had poor mechanical properties and a coarse morphology because of their poor interfacial adhesion. A major concern in designing polymer blends with useful properties is the relationship between polymer structure and blend thermodynamics. The interaction energy between unlike polymer pairs is a fundamental thermodynamic issue that governs the state of miscibility of their blends or the natures of the interface when the blend is phase separated [3–5].

Bisphenol-A polysulfone (PSf) is an engineering thermoplastic with exceptional mechanical properties [6–10]. It is a transparent, rigid, tough thermoplastic with high glass transition and chemical inertness. It also has excellent hydrolytic stability and its ability to retain mechanical properties in hot, wet environments. Because of these properties, PSf is being widely used in the membrane area such as supports for composite membrane, ultrafilitration membrane, and gas separation membrane. However, application of PSf membrane often limited because of its hydrophobic nature. Hydrophobic interaction between PSf and hydrophobic solute in feed solution often caused serious membrane fouling, and then deteriorate membrane performance. Moreover, since hydrophobic membranes are non-wettable by water, a relative high-pressure gradient is required to pass water through the membrane pores. Thus, membranes having hydrophilic properties are desirable. Introduction of hydrophilic property to the PSf membrane is critical to maintain excellent membrane performance in the long time application. The hydrophilic properties can be endowed to the PSf by blending with hydrophilic polymers. PSf blend with hydrophilic polymers should be miscible or nearly miscible for the membrane application because interface having poor adhesion acts as defects of membrane. Blending of

* Corresponding author. Tel.: +82 2 820 5324; fax: +82 2 824 3496.
E-mail address: ckkim@cau.ac.kr (C.K. Kim).

0032-3861/$ - see front matter © 2005 Elsevier Ltd. All rights reserved.
doi:10.1016/j.polymer.2005.03.108

polysulfones with other polymers has been studied extensively [11–15]. Recently, we had found that PSf (or polyethersulfone) formed miscible blends with poly(1-vinylpyrrolidone-*co*-styrene) copolymers (P(VP–S)) containing certain amount of VP [14,15]. Except these blends, miscible PSf blends with hydrophilic polymers were not known as far as we know to date. However, hydrophilicity of these blends was not strong enough because of hydrophobic nature of styrene unit involved in copolymers.

Since polyacrylonitrile (PAN) has better hydrophilicity than polystyrene, one can expect better hydrophilic copolymer by incorporating AN instead of styrene. Furthermore, according to a binary interaction model for describing how the net interaction energy depends on copolymer composition [16–18], copolymerization can be an effective strategy to produce a new miscible blend even though neither homopolymer PVP or PAN is miscible with PSf. Based on this, poly(1-vinylpyrrolidone-*co*-acrylonitrile) (P(VP–AN)) containing various amounts of AN were synthesized and then blended with PSf to produce miscible blends that could be used for the fabrication of membrane exhibiting excellent performance.

Miscibility of polymer blends is often judged from specimens prepared by melt blending or solution casting methods. However, an inappropriate choice of temperature or solvent may lead to an erroneous judgment about miscibility owing to phase separation result from LCST-type (lower critical solution temperature-type) phase behavior or the so-called solvent effect [19–22]. Blend samples were prepared by solvent casting. Since miscibility of blends examined here was sensitive to the preparation methods, various solvent casting methods were used to prepare blend samples. When prepared samples are transparent and show a single glass transition, phase separation temperatures caused by LCST-type phase behavior were examined. The binary interaction energies involved in the miscible blends were quantified from the LCST type phase boundaries using lattice–fluid theory [23–26] combined with binary interaction model [16–18]. The effects of intermolecular interactions and compressibility of these blends on miscibility and phase behavior were also discussed.

2. Background

Flory–Huggins theory [27,28] is widely used to describe the thermodynamic properties for a variety of polymer systems. The free energy of mixing per unit volume, g, can be expressed in terms of the classical Flory–Huggins theory as follows

$$\Delta g_{\mathrm{m}} = \Delta g_{\mathrm{nc}} + \Delta g_{\mathrm{c}} \tag{1}$$

where Δg_{c} is the combinatorial entropy

$$\Delta g_{\mathrm{c}} = RT\left(\frac{\phi_1 \ln \phi_1}{\tilde{V}_1} + \frac{\phi_2 \ln \phi_2}{\tilde{V}_2}\right) \tag{2}$$

and Δg_{nc} is the non-combinatorial free energy represented by the Van-Laar form Refs. [5,29]

$$\Delta g_{\mathrm{nc}} = B\phi_1\phi_2 \tag{3}$$

The ϕ_i and $\tilde{V}_i$ are the volume fraction and molar volume of component i, respectively, and B is the interaction energy density.

The combinatorial entropy always favors mixing. If the interaction parameter is negative then, according to this theory, all binary compositions are miscible at all temperatures. When B is independent of temperature, this theory only predicts UCST type behavior. If B is a function of temperature, basic thermodynamic relations reveal that this quantity is not strictly an enthalpic parameter but also contains a non-combinatorial entropic contribution. An empirical excess entropy term $-TS^{\mathrm{E}} = -TB^{\mathrm{S}}\phi_1\phi_2$ is often added to Eq. (3), which enables the theory to describe LCST behavior. In this extended Flory–Huggins theory, the interaction parameter takes on the form

$$B(T) = B^{\mathrm{h}} - TB^{\mathrm{S}} \tag{4}$$

If the interaction energy density in Eq. (3) does not depend on ϕ_i, simple differentiation of Eqs. (1)–(3) leads to the familiar spinodal condition

$$\frac{\mathrm{d}^2\Delta g}{\mathrm{d}\phi_1^2} = RT\left(\frac{1}{\phi_1\tilde{V}_1} + \frac{1}{\phi_2\tilde{V}_2}\right) - 2B_{\mathrm{SC}} = 0 \tag{5}$$

This form is often used even though the interaction energy does depend on ϕ_1.

Thus, Eq. (5) amounts to the definition of a interaction energy, i.e.

$$B_{\mathrm{SC}} = -\frac{1}{2}\frac{\mathrm{d}^2\Delta g_{\mathrm{nc}}}{\mathrm{d}\phi_1^2} \tag{6}$$

to which we add the subscript SC, following the notation of Sanchez [30], in order to distinguish it from B in Eq. (3). In general, interaction energies defined by Eqs. (1)–(3), (5), or other free energy derived equations are not identical but interrelated as shown by Sanchez, e.g.

$$B_{\mathrm{SC}} = B(T) + (\phi_1 - \phi_2)\frac{\mathrm{d}B(T)}{\mathrm{d}\phi_1} - \frac{1}{2}\phi_1\phi_2\frac{\mathrm{d}^2B(T)}{\mathrm{d}\phi_1^2} \tag{7}$$

The interaction parameters used here have units of energy/volume and differ by the factor RT from the χ quantities used by Sanchez.

The Flory–Huggins theory does not account for the compressible nature of the pure components or mixture. Furthermore, it assumes mixing to occur without change in volume, which, of course, is only an approximation to how real system behave. This latter assumption is often mistakenly considered to be an important factor in phase behavior. Rather, it is the finite compressibility, together with any mismatch in pure component equation-of-state properties, which affect the solution properties of a blend. Equation of state theories have emerged to account for these

effects [23–26,31–33]. Basically, these theories expand the elements of the Flory–Huggins theory by introducing contributions to the entropy and enthalpy of mixing resulting from free volume considerations. These theories predict LCST behavior without resorting to the empiricism used in Eq. (4). These theories can be forced into the Flory–Huggins form to obtain their predicted expressions for B, B_{SC}, and the other interaction parameters described by Sanchez. These expressions naturally depend on temperature and composition. It is appealing to attribute the experimentally observed temperature and composition dependence of the Flory–Huggins type interaction parameters to equation-of-state effects, and that is an assumption that we make here. However, it should be recognized that other mechanisms could contribute to the dependence on T and ϕ. There are several equation of state theories for mixtures; however, the following discussion is limited to the lattice–fluid theory of Sanchez and Lacombe [23–26]. This theory expresses thermodynamic functions in terms of reduced variables $\tilde{P}=P/P^*$, $\tilde{T}=T/T^*$, $\tilde{\rho}=1/\tilde{V}=\rho/\rho^*=v^*_{sp}/v_{sp}$, where the asterisks denote characteristic parameters. The free energy per unit hard core volume is given by

$$\frac{G}{V^*}=g_{nc}+g_c \tag{8}$$

where

$$g_{nc}=-\tilde{\rho}P^*+P\tilde{V}+\frac{kT}{V^*}\left(1-\tilde{\rho}\tilde{\rho}\ln(1-\tilde{\rho})+\frac{\ln\tilde{\rho}}{r}\right) \tag{9}$$

and

$$g_c=\frac{kT}{V^*}\sum_i\frac{\phi}{r_i}\ln\phi_i \tag{10}$$

Chain length, r, is given by $r=MP^*/RT^*\rho^*$ where M is the molecular weight (weight average should be used for polydisperse components). The enthalpy of mixing ΔH_m at low pressure for a binary mixture is given by

$$\frac{\Delta H_m}{V}=\tilde{\rho}^2\Delta P^*\phi_1\phi_2+\tilde{\rho}[\phi_1P_1^*(\tilde{\rho}_1-\tilde{\rho})+\phi_2P_2^*(\tilde{\rho}_2-\tilde{\rho})] \tag{11}$$

The characteristic pressure for the mixture, P^*, is related to those of the pure components, P_i^*, and the bare interaction energy, ΔP^*, by

$$P^*=\phi_1P_1^*+\phi_2P_2^*-\phi_1\phi_2\Delta P^* \tag{12}$$

where the ϕ_i are close-packed volume fractions. The reduced density $\tilde{\rho}$ refers to the mixture, whereas $\tilde{\rho}_i$ refers to the pure components. Eq. (11) allows for the effects of finite compressibility on the enthalpy of mixing. Interaction parameters defined in the extended Flory–Huggins theory can be simply expressed in terms of equation of state parameters by assuming the ϕ_i used in the two theories are essentially equal. From Eqs. (4) and (11), the interaction energy related to the heat of mixing, B^h, is by

$$B^h=\tilde{\rho}\Delta P^*+\left[\frac{p_1^*}{\phi_2}(\tilde{\rho}_1-\tilde{\rho})+\frac{P_2^*}{\phi_1}(\tilde{\rho}_2-\tilde{\rho})\right] \tag{13}$$

A relationship for the excess entropy term, $-TB^S$, can be similarly derived

$$-TB^S=\frac{RT}{\phi_1\phi_2}\left\{\frac{1}{V^*}\left[1-\tilde{\rho}\tilde{\rho}\ln(1-\tilde{\rho})+\frac{\ln\tilde{\rho}}{r}\right]-\frac{\phi_1}{V_1^*}\left[\frac{1-\tilde{\rho}_1}{\tilde{\rho}_1}\ln(1-\tilde{\rho}_1)+\frac{\ln\tilde{\rho}_1}{r_1^0}\right)\right]-\frac{\phi_2}{V_2^*}\left[\frac{1-\tilde{\rho}_2}{\tilde{\rho}_2}\ln(1-\tilde{\rho}_2)+\frac{\ln\tilde{\rho}_2}{r_2^0}\right]\right\} \tag{14}$$

Finally, the spinodal condition for a compressible mixture can be written

$$\frac{d^2g}{d\phi^2}=g_{\phi\phi}-\frac{(g_{\tilde{\rho}\phi})^2}{g_{\tilde{\rho}\tilde{\rho}}}=0 \tag{15}$$

where the subscripts ϕ and $\tilde{\rho}$ indicate partial derivatives with respect to ϕ or $\tilde{\rho}$. In terms of the Sanchez-Lacombe theory, the indicated derivatives for binary mixture are given by

$$g_{\phi\phi}=-2\tilde{\rho}\Delta p^*+RT\left(\frac{1}{\phi_1r_1v_1^*}+\frac{1}{\phi_2r_2v_2^*}\right) \tag{16}$$

$$g_{\tilde{\rho}\phi}=-(P_1^*-P_2^*-(1-2\phi_1)\Delta P^*)+RT\tilde{\rho}\left(\frac{1}{r_1v_1^*}-\frac{1}{r_2v_2^*}\right)-RT\left(\frac{1}{v_1^*}-\frac{1}{v_2^*}\right)\left(\frac{\ln(1-\tilde{\rho})}{\tilde{\rho}^2}+1\tilde{\rho}\right) \tag{17}$$

$$g_{\tilde{\rho}\tilde{\rho}}=\frac{RT}{v^*}\left(\frac{2\ln(1-\tilde{\rho})}{\tilde{\rho}^3}+\frac{1}{\tilde{\rho}^2(1-\tilde{\rho})}+\frac{1}{\tilde{\rho}^2}\left(1-\frac{1}{r}\right)\right) \tag{18}$$

From Eqs. (6) and (15), the following expression for B_{SC} is obtained

$$B_{SC}=\frac{\tilde{\rho}\Delta P^*+\left\{[P_2^*-P_1^*+(\phi_2-\phi_1)\Delta P^*]+RT\tilde{\rho}\left(\frac{1}{r_1^0V_1^*}-\frac{1}{r_2^0V_2^*}\right)-RT\left(\frac{\ln(1-\tilde{\rho})}{\tilde{\rho}^2}+1\tilde{\rho}\right)\left(\frac{1}{V_1^*}-\frac{1}{V_2^*}\right)\right\}^2}{\left\{\frac{2RT}{V^*}\left[\frac{2\ln(1-\tilde{\rho})}{\tilde{\rho}^3}+\frac{1}{\tilde{\rho}^2(1-\tilde{\rho})}+\frac{1-1/r}{\rho^2}\right]\right\}} \tag{19}$$

A binary interaction model [16–18], in which the heat of mixing, the primary governing factor, is determined by a combination of interactions between units in each of the

polymers being mixed, offers the potential or making a priori prediction about the phase behavior of a mixture of two polymers. This model envisions each polymer as being comprised of structural units. Note that the model treatment can be also used for units smaller than monomer or structural unit. The interaction between unlike units i and j within the blend or in polymer itself is characterized by the product of an interaction energy density B_{ij} and the volume fraction of these units, regardless of to what they may be covalently bonded. Thus the heat of mixing a volume V_A of polymer A and a volume V_B of polymer B is given by

$$\frac{\Delta H_m}{V} = B\phi_A\phi_B \tag{20}$$

$$\frac{\Delta H_m}{V} = \sum_{i>j}^{\text{blend}} B_{ij}\phi_i\phi_j - \frac{V_A}{V}\sum_{k>l}^{A} B_{kl}\phi'_k\phi'_l - \frac{V_B}{V}\sum_{m>n}^{B} B_{mn}\phi''_m\phi''_n \tag{21}$$

where each summation is over unlike pairs without double counting; ϕ_i gives the concentration of units i in the blend, ϕ'_k the concentration of unit k in A, and ϕ''_m the concentration of unit m in B. The overall interaction parameter B can be expressed in terms of B_{ij} and the composition of polymers A and B. A random copolymer (polymer A) composed of units 1 and 2 units and a homopolymer (polymer B) of 3, the overall interaction parameter is given by

$$B = B_{13}\phi'_1 + B_{23}\phi'_2 - B_{12}\phi'_1\phi'_2 \tag{22}$$

where ϕ'_i describe the copolymer composition. For the case above both B_{13} and B_{23} would be positive. If B_{12} is a large enough positive value, B can be negative over certain range of copolymer composition. This occurs because addition of polymer 3 to the copolymer dilute the unfavorable interactions between 1 and 2, causing a net exothermic mixing condition even though no individual binary interaction is exothermic. Thus, intrachain repulsion can be a driving force for miscibility even when no strong specific interactions are involved. The bare interaction energy, ΔP^*, in Eqs. (11) and (12) between copolymer and homopolymer is assumed to be given by [34]

$$\Delta P^* = \Delta P^*_{13}\phi'_1 + \Delta P^*_{23}\phi'_2 - \Delta P^*_{12}\phi'_1\phi'_2 \tag{23}$$

3. Materials and procedure

The polymers used in this study are listed in Table 1. Commercially available PSf (grade: Udel P-3500) and polyvinylpyrrolidone (PVP) having various molecular weights were purchased from Amoco performance Products Inc. and Aldrich Chemical Co, respectively. P(VP–AN) copolymers were synthesized at various copolymer compositions in our laboratory. Copolymerization was performed in the bulk at 80 °C with AIBN (Azobis(isobutyronitrile)) as the initiator and ethyl benzene as the chain transfer agent. Conversion was kept less than 10% to avoid composition drift in the copolymer. The resulting solution was poured into a large excess of n-hexane to precipitate the polymer. Weight average molecular weights of copolymers were measured by light scattering. Copolymer composition was determined by element analysis. The numerical value included as part of the code for these copolymers indicates the weight percent of AN. The reactivity ratio is an indication of the preference of a growing chain for adding a monomer identical to the terminal unit or for adding the other monomer. The reactivity ratios of VP and AN, i.e. r_{VP} and r_{AN} are known 0.06 and 0.18, respectively [35]. The reactivity ratios being known, the instantaneous and average copolymer compositions could be calculated as a function of conversion for different compositions of the initial monomer mixture. Since at about 10% conversion, the instantaneous copolymer composition remained fairly close to its initial value, composition drift could be avoided. Copolymer composition determined by element analysis agreed with the calculated composition with an average relative error of ca. 10%. The synthetic procedure used here might yield as nearly random structures as the relative reactivities of the monomer permit.

Blends were prepared from three different methods coded P_1, P_2, and P_3. The details of each are described below. P_1: the blend was prepared in film form by casting solutions containing 5 wt% total polymer in dichloromethane onto petri dish at room temperature. After slow drying at room temperature for a day, the blends were finally dried in a vacuum oven at 120 °C for a week. P_2: this method followed the same procedure as P_1 except that the solvent was 1-methyl-2-pyrrolidone (NMP) and then solvent was evaporated at 100 °C. P_3: in this method, PSf and copolymer were precipitated simultaneously from the NMP solution using the non-solvent n-hexane. The precipitate was allowed to dry in an air-circulating oven and then further dried in a vacuum oven at 120 °C for a week.

Glass transition temperatures were measured at a heating rate of 20 °C/min by using DSC (TA Instrument, model DSC-2010). The first scan was run to 190 °C to erase previous thermal history during sample preparation, and then the sample was quenched to room temperature to start the second scan. The glass transition temperature, T_g, was defined as the onset of change in the heat capacity during the second heating from room temperature to 230 °C. The phase separation temperature caused by the lower critical solution temperature (LCST) type phase behavior was measured by an annealing technique to access the closet true equilibrium temperature [15,36,37].

For evaluation of the hydrophilicity the contact angle between water and the blend film was determined. The contact angle, θ, between water and the blend film was directly measured using a contact angle goniometer (Rame-Hart, Model 100-00-(115/220)-S). To minimize experimental error, the contact angle was measured ten times for each

Table 1
Polymers used in this study

Abbreviation[a]	$\bar{M}_W$	T_g (°C)	Source
PSf	69,000[b]	189	Amoco, Udel P-3500
P(VP–AN) 55	–	145	Synthesized
P(VP–AN) 50	–	151	Synthesized
P(VP–AN) 33	–	153	Synthesized
P(VP–AN) 22	155,000[c]	155	Synthesized
P(VP–AN) 16	184,000[c]	157	Synthesized
P(VP–AN) 10	16,5000[c]	158	Synthesized
P(VP–AN) 8	192,000[c]	160	Synthesized
P(VP–AN) 5	178,000[c]	167	Synthesized
P(VP–AN) 2	185,000[c]	175	Synthesized
PVP(10K)	10,000[b]	129	Aldrich
PVP(30K)	30,000[b]	155	Aldrich
PVP(55K)	55,000[b]	157	Aldrich

[a] The numerical value included as part of the code for these copolymers indicates the weight percent of AN.
[b] Molecular information was provided by supplier.
[c] Molecular weights were determined by light scattering.

sample and then averaged. The work of adhesion of dispersion for polymers is given by [38]:

$$\omega_A = \gamma_W(1 + \cos\theta) \quad (24)$$

where γ_W is water surface tension $= 7.28 \times 10^{-2}$ N/m. Values of ω_A for different membranes indicate their hydrophilicity.

4. Results and discussion

4.1. Miscibility of blends

An inappropriate choice of solvent may lead to an erroneous judgment about miscibility owing to the so-called solvent effect [19–22]. Since miscibility of blends examined here was sensitive to the preparation methods, various solvent casting methods were used to prepare blend samples. Fig. 1 shows DSC thermograms of PSf/P(VP–AN) 5 = 5/5 blends prepared by two different preparation methods. The blend cast from dichloromethane (method P_1) was translucent and visually heterogeneous, and DSC thermogram revealed two glass transitions (Fig. 1(a)). However, the PSf/P(VP–AN) 5 = 5/5 blend cast from NMP (method P_2) was transparent, and its thermogram revealed a single T_g (Fig. 1(b)). Note that blends prepared by method P_3 exhibited the same T_g behavior with those prepared by method P_2. Because of this, blend samples prepared by method P_2 were used for further study. Fig. 2

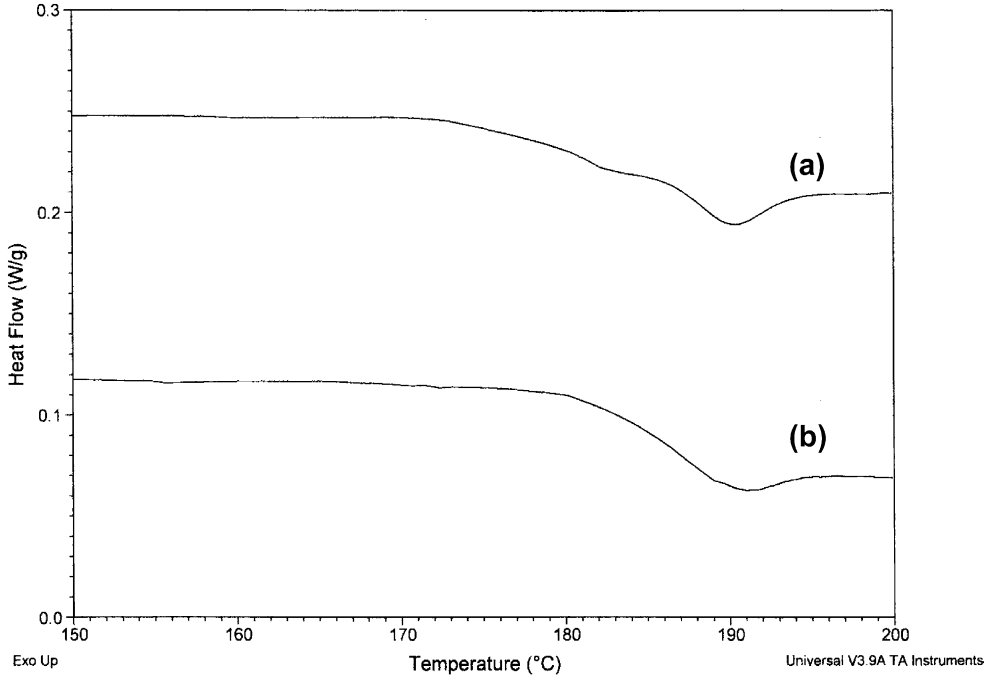

Fig. 1. DSC thermograms for PSf/P(VP–AN) 5 = 5/5 blends; (a) cast from dichloromethane at room temperature; (b) cast from NMP at 100 °C.

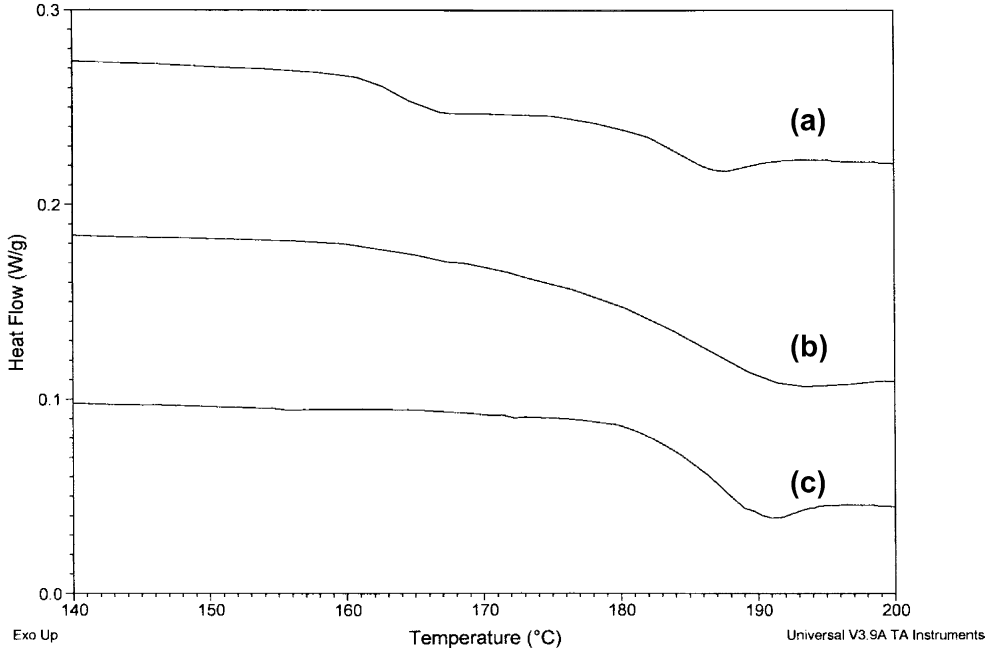

Fig. 2. DSC thermograms for PSf/P(VP–AN) = 5/5 blends; (a) PSf/P(VP–AN) 33; (b) PSf/P(VP–AN) 22; (c) PSf/P(VP–AN) 5.

shows the selected DSC thermograms of PSf blends with the P(VP–AN) copolymers containing various amount of AN. Blends of PSf with copolymers containing AN from 2 to 16 wt% were transparent and showed a single T_g, while PSf blends with P(VP–AN) copolymers containing more than 22 wt% AN were opaque and showed two T_gs indicating that phase separation occurred. From these results, it was concluded that PSf/P(VP–AN) blends of casting from NMP formed miscible when copolymers contain AN from 2 to 16 wt% but beyond these critical limits to form immiscible blends.

It was known that PSf did not form miscible blends with PVP [7–11,14,15]. According to our previous research [14], PSf/PVP binary pair had small positive interaction energy, i.e. 0.1 cal/cm^3. When immiscible polymer pair has small positive interaction energy, decreasing the molecular weight of one or both components can lead to miscibility. Various PSf/PVP blends were prepared by changing molecular weights of PVP and then changes in their glass transition temperatures were examined. Note that blends were prepared by method P_2. The blends of PSf/PVP (55 K) and PSf/PVP (30 K) were slightly cloudy and showed two T_gs (see Fig. 3(a) for PSf/PVP (30 K) = 5/5 blend). However, PSf/PVP (10 K) blends were transparent at all compositions and exhibited a single T_g (see Fig. 3(b) for PSf/PVP (10 K) = 5/5 blend). The T_gs for PSf/PVP (10 K) blends were found to lie between T_gs of pure components and were well approximated by the Fox equation [39]. The results indicated that PSf blends with PVP were not miscible but appeared to be right on the edge of being so.

As reported previously, when blend is near the boundary of miscibility window, miscibility of blend prepared by solvent casting often does not reflect an equilibrium phase behavior because of slow kinetics of phase separation [36,40,41]. To avoid misleading results in judging the miscibility of blends observed here, isothermal annealing for the blends exhibiting single T_g behavior was performed at a temperature 20 °C higher than the measured T_g for 1 week to observe whether phase separation occurs or not. Blend samples were still transparent and exhibited a single T_g after annealing. With these results, it was concluded that blends exhibiting a single T_g were miscible at equilibrium state. As summary, PSf did not formed miscible blend with PVP when both components had high molecular weight, while it formed miscible blends with P(VP–AN) copolymers containing from 2 to 16 wt% AN.

4.2. Phase separation of blends

Phase separation temperature of blends caused by LCST-type phase behavior was measured by an annealing technique. For example, the PSf/P(VP–AN) 5 = 5/5 blend was heated rapidly to a temperature about 180 °C and then heated at a rate of 2 °C/min. Changes in the image with temperature were observed as the specimens were heated at a rate of 2 °C/min. Changes in the image were observed at 223 °C. After determining the temperature at which phase separation occurred, blend specimens were annealed in the hot stage at a fixed temperature for 1 h. Fig. 4 shows the image analyzer photography of same blend after being annealed at 215 and 225 °C. The blend annealed at 215 °C was still clear and changes in the morphology of the blend were not observed while that annealed at 225 °C became opaque and changes in the morphology were observed during annealing. The phase boundary would appear to lie between 215 and 225 °C for this blend. By successively

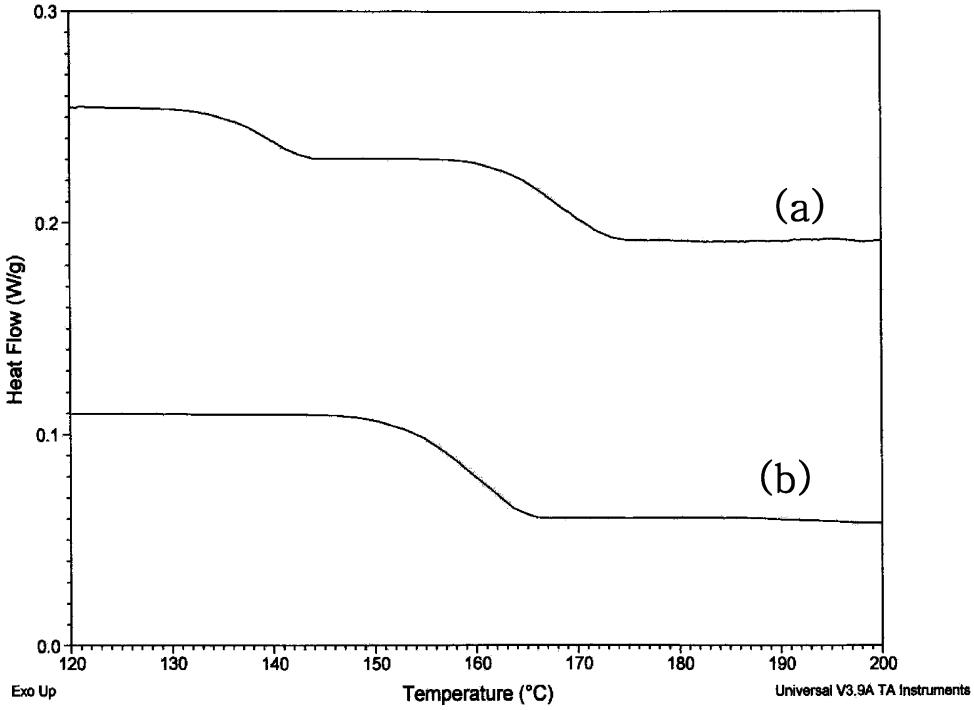

Fig. 3. DSC thermograms for PSf/PVP = 5/5 blends; (a) PSf/PVP (30k) blend; (b) PSf/PVP (10k) blend.

repeating annealing process within the measured temperature range, the location of the phase boundary was determined.

Miscible blends observed here exhibited LSCT-type phase behavior. Fig. 5 showed phase separation temperatures for PSf/PVP (10 K) blends, while Fig. 6 exhibited those for PSf/P(VP–AN) miscible blends. The phase separation temperature curves for PSf/P(VP–AN) miscible blends were all very similar with each showing a minimum at about 50 wt% PSf. The effect of AN content can be exhibited more easily with a plot of the phase separation temperature for a fixed PSf content of the blend versus the AN content of the copolymer, as shown in Fig. 7. The phase separation temperature of miscible blends first increased with AN content, went through a maximum centered at about 8 wt% AN and then decreased just prior to the limiting content of AN for miscibility with PSf.

4.3. Interaction energies and phase behavior

To understand the phase behavior of blends, interaction energies of binary pairs involved in the PSf/P(VP–AN) blends were calculated from the phase boundary using the lattice–fluid theory combined with binary interaction model. To extract information about interaction energy from the liquid–liquid phase boundaries, it is assumed that to a good approximation these data correspond to the spinodal curve. The morphology of the blends observed with an image analyzer at the reported phase separation temperature could be also characterized by a high level of phase interconnectivity in both the minor and major phase caused by spinodal decomposition [15,36,37,42,43]. For the evaluation of the interaction energies responsible for the equilibrium phase behavior using an equation-of-state theory, characteristic parameters of polymers are required. Pressure–volume–temperature data for each polymeric component are required so that characteristic parameters can be determined. The characteristic parameters of PSf, PAN, and PVP obtained from the pressure-volume-temperature data were listed in Table 2 and those of P(VP–AN) were obtained by using the mixing rule [12,14,42].

Bare interaction energy between PSf and PVP, i.e. $\Delta P^*_{\mathrm{PSf–PVP}}$, was calculated form phase boundary of PSf/PVP (10k) shown in Fig. 6 using Eq. (15). The $\Delta P^*_{\mathrm{PSf–PVP}}$ values so obtained for blends of PSf with PVP were essentially composition independent as described in the lattice–fluid theory. The obtained $\Delta P^*_{\mathrm{PSf–PVP}}$ value was 0.05 cal/cm^3. This value, i.e. small positive value indicated that immiscible PSf/PVP blend will become miscible by reducing molecular weight of one or both components as observed above.

Interaction energies between PSf and P(VP–AN), i.e. $\Delta P^*_{\mathrm{PSf–P(VP–AN)}}$ were also calculated from phase boundaries of miscible PSf blends with P(VP–AN) copolymers.

Table 2
Characteristic properties of polymers in the lattice–fluid theory

Abbreviation	T^* (K)	P^* (bar)	ρ^* (g/cm^3)	References
PSf	852	5948	1.3017	[12]
PAN	853	5357	1.2299	[31]
PVP	810	5650	1.0904	[14]

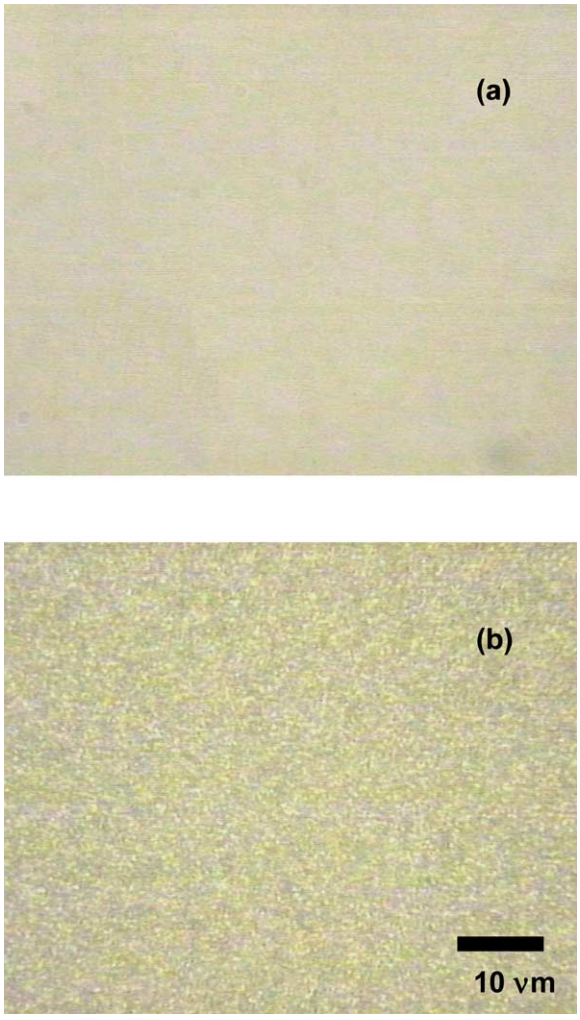

Fig. 4. The image analyzer photography of PSf/P(VP–AN) 95 = 5/5 blend annealed at 215 and 225 °C, respectively: (a) annealed at 215 °C, (b) annealed at 225 °C.

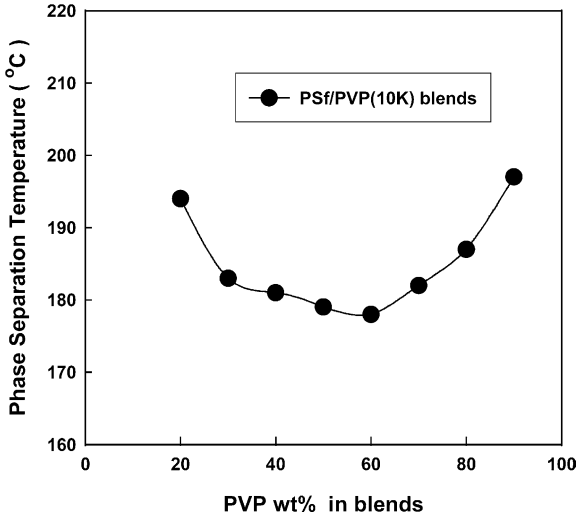

Fig. 5. Phase separation temperatures of PSf blends with PVP (10k).

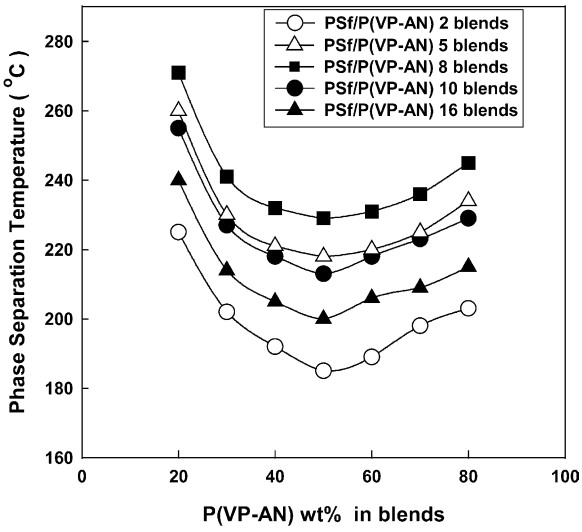

Fig. 6. Phase separation temperatures of PSf blends with various P(VP–AN) copolymers.

The $\Delta P^*_{PSf-P(VP-AN)}$ values so obtained for blends of PSf with specific P(VP–AN) copolymers were also composition independent essentially. Fig. 8 exhibited changes in the $\Delta P^*_{PSf-P(VP-AN)}$ as a function of copolymer composition. Fig. 9 shows experimental phase separation temperatures of the PSf/P(VP–AN) 10 blends and the spinodal curve calculated from Eq. (15) using a constant interaction energy for the corresponding blend ($\Delta P^*_{PSf-P(VP-AN)10} = -0.06$ cal/cm^3). The curves agree with the experimentally determined phase separation temperatures. Interaction energies of the binary pairs involved in PSf/P(VP–AN) blends, i.e. ΔP^*_{PSf-AN} and ΔP^*_{VP-AN} were extracted from $\Delta P^*_{PSf-P(VP-AN)}$ values using Eq. (23). Note that $\Delta P^*_{PSf-PVP} = 0.05$ cal/cm^3 was used for this calculation. Large positive values of $\Delta P^*_{PSf-AN} = 7.0$ cal/cm^3 and $\Delta P^*_{VP-AN} = 8.8$ cal/cm^3 indicated that polymer blends composed of these binary pairs were immiscible.

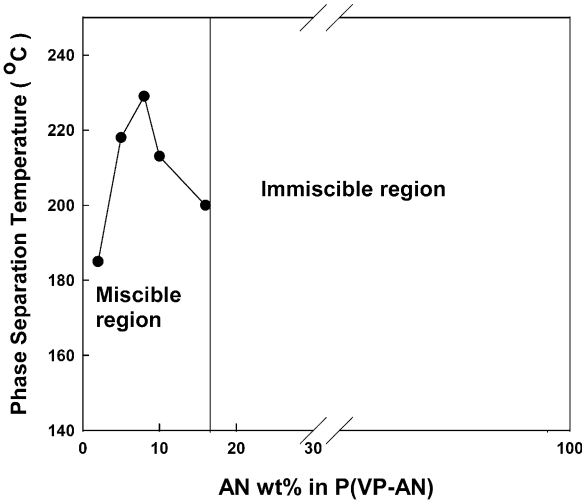

Fig. 7. Miscibility map and phase separation temperatures for 50/50 blends of PSf with P(VP–AN) copolymers.

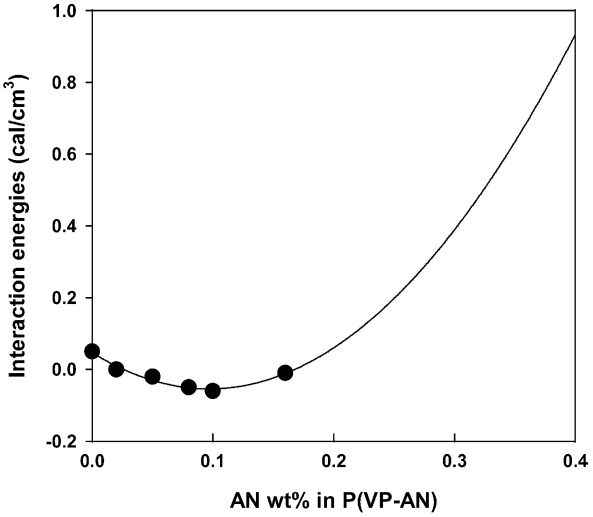

Fig. 8. Changes in the interaction energies of PSf/P(VP–AN) blends as a function of AN content in P(VP–AN) copolymers.

Interaction energies of three binary pairs obtained here are positive. Specific interactions between amide group in PVP and sulfonyl group in PSf are not strong enough to result in miscible blends of PSf and PVP (or P(VP–AN)). However, as described in a binary interaction model, if ΔP^*_{VP-AN} is a large enough positive value, interaction energy between PSf and P(VP–AN), $\Delta P^*_{PSf-P(VP-AN)}$, can be negative over a certain range of copolymer composition (Fig. 8). Many examples are known where a random copolymer comprised monomers 1 and 2 is miscible with a homopolymer comprised of monomer 3, even though neither homopolymer 1 or 2 is miscible with homopolymer 3 [14,15,44–46]. Since addition of polymer PSf to the P(VP–AN) copolymer dilute the highly unfavorable interaction between VP and AN, a net exothermic mixing could be expected between PSf and P(VP–AN) at a certain copolymer composition. Thus it could be concluded that strong intrachain repulsion between VP and AN is a driving force for miscibility of PSf/P(VP–AN) blends.

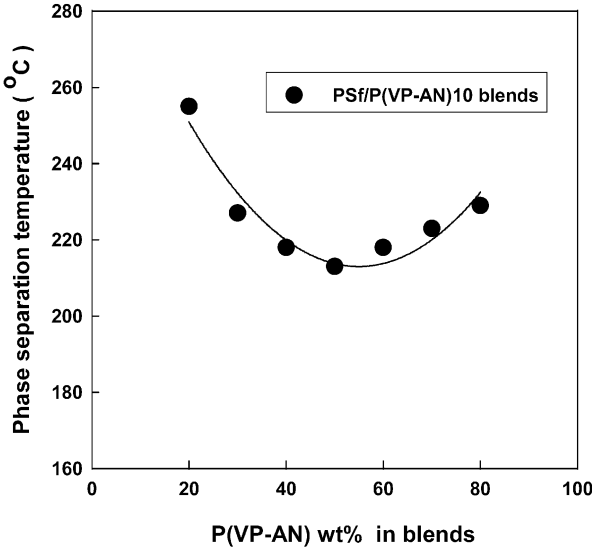

Fig. 9. Experimental phase separation temperatures of PSf/P(VP–AN) 10 blends. Note that the corresponding spinodal curves were calculated from Eq. (4) with interaction energies obtained here.

To understand phase separation behavior of PSf and P(VP–AN) blend, the phase stability condition of lattice–fluid theory was analyzed. For the phase stability, the term in Eq. (15), i.e. $d^2g/d\phi^2$ should be positive. The indicated derivatives in Eqs. (16)–(18) are approximately given by [42]

$$\frac{d^2g}{d\phi^2} \approx -2\tilde{\rho}\Delta P^* - \left(\frac{R}{v^*}\right)^2 (T^*_{PSf} - T^*_{P(VP-AN)})^2 \kappa \tilde{\rho}^3 > 0 \quad (25)$$

where ΔP^* is bare interaction energy between PSf and P(VP–AN) copolymer, T^*_{PSf} and $T^*_{P(VP-AN)}$ are characteristic temperature of PSf and P(VP–AN) copolymer, respectively, and κ is the isothermal compressibility of the binary mixture. Note that the combinatorial entropy terms are negligible at high molecular weight. The explanation for the observed phase behavior of blends is revealed in the two terms of Eq. (25) comprising the stability condition. Since the characteristic temperature for PAN is larger than that for PVP, the characteristic temperature for P(VP–AN) copolymer ($T^*_{P(VP-AN)}$) become larger as AN content increases. The difference in the characteristic temperature, $|T^*_{PSf} - T^*_{P(VP-AN)}|$, becomes larger as the VP content of the copolymer increases (Table 2). The contribution of this term to the phase stability becomes less favorable as VP content increases. Since the reduced density becomes smaller as VP content increases, at a given temperature, a smaller reduced density results in a larger isothermal compressibility of the copolymer. The increased compressibility and the increased interaction energy (ΔP^*) destabilize the mixture and promote phase separation. In consequence, compressibility

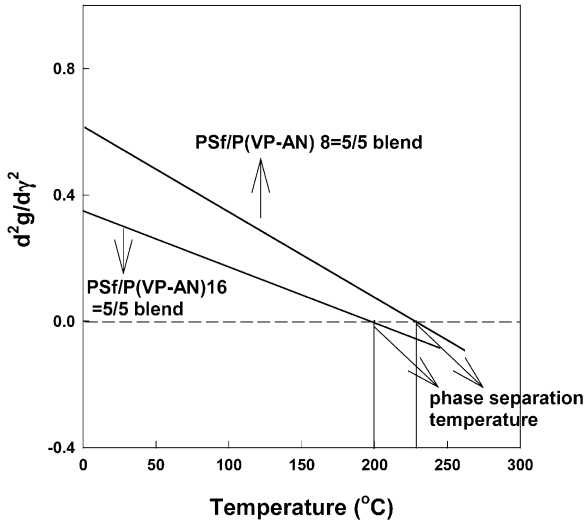

Fig. 10. Changes in $d^2g/d\phi^2$ of PSf/P(VP–AN)=5/5 blends with temperature.

and the difference in the characteristic temperature become less favorable for phase stability as VP content increases, while interaction energies depend on the copolymer composition. To see this more clearly, $d^2g/d\phi^2$ was plotted as a function of temperature. Fig. 10 showed the calculated $d^2g/d\phi^2$ of two different PSf/P(VP–AN) blends as a function of temperature. It was suggested that the increased compressibility with temperature results in phase separation of PSf/P(VP–S) blends and their phase boundaries are determined by the competition among these terms.

4.4. Contact angle

The contact angle studies were conducted to assess changes in hydrophilicity as P(VP–AN) copolymer is incorporated into the blend film. Fig. 11 showed the contact angle values and the adhesion work of PSf/P(VP–AN) 16 blends at various compositions. The decline in the contact angle, i.e. the increase in the adhesion work was observed by increasing P(VP–AN) 16 content. The results obtained here indicated that the hydrophilic properties could be endowed to the PSf by blending with P(VP–AN) copolymers and these blends might be used for the fabrication of membranes exhibiting excellent performance.

5. Summary

The miscibility of PSf blends with P(VP–AN) copolymers containing various amounts of AN and that of PSf blends with PVP were examined. Even though PSf/PVP blend were not miscible when both components had high molecular weights, this blend became miscible by reducing molecular weight of PVP. It meant that PSf blends with PVP were not miscible but appeared to be right on the edge of being so. Copolymers composed of VP and AN were prepared to produce miscible blends with PSf. The miscibility of PSf/P(VP–AN) blends was affected by preparation method of blend. On the basis of the T_g behavior and the phase separation temperatures caused by LCST-type phase behavior, it was concluded that copolymer of P(VP–AN) containing between 2 and 16 wt% AN gave homogeneous mixtures. The phase separation temperature of miscible blends first increased with AN content, went through a maximum centered at about 8 wt% AN and then decreased just prior to the limiting content of AN for miscibility with PSf. To understand phase behavior of blends examined here, interaction energies were calculated from phase boundaries using lattice–fluid theory combined with binary interaction model. The results indicated that the miscibility of PSf with P(VP–AN) copolymers stemmed from strong intrachain repulsion between VP and AN even though interaction energies of binary pairs involved in PSf/P(VP–AN) blend are positive. Spinodal temperatures predicted from the lattice–fluid theory with interaction energies obtained here were similar to the experimental phase separation temperatures. It also confirmed that the increased compressibility with temperature results in phase separation of blends on heating.

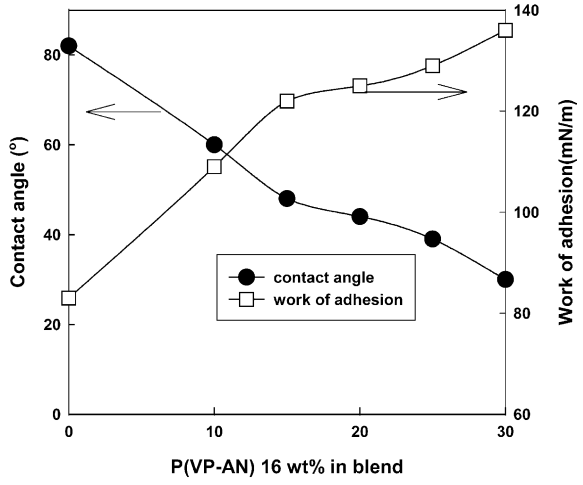

Fig. 11. The contact angles (or works of adhesion) between water and blend films as a function of P(VP–S) 16 content.

Acknowledgements

This work was supported by the research grant from KOSEF (grant number: ROI-2003-000-10216-0).

References

[1] Paul DR, Bucknall CB. In: Paul DR, Bucknall CB, editors. Polymer blends, vol. 1. New York: Wiley; 1999 [chapter 1].
[2] Paul DR, Walsh DJ, Higgins JS. In: Maconnachie A, editor. Polymer blends and mixtures. NATO ASI series E, applied science, vol. 89. Dordrecht: Martinus Nijoff Publishers; 1985. p. 1.
[3] Olabisi O, Robenson LM, Shaw MT. Polymer–polymer miscibility. New York: Academic Press; 1979 [chapters 2–3].
[4] Freitag D, Grigo U, Muller PR, Nouvertne W. In: Mark HF, Bikales NM, Overberger CG, Menges G, editors. Encyclopedia of polymer science and engineering, 2nd ed, vol. 11. New York: Wiley; 1988. p. 48.
[5] Paul DR, Barlow JW, Keskkula H. In: Mark HF, Bikales NM, Overberger CG, Menges G, editors. Encyclopedia of polymer science and engineering, 2nd ed, vol. 12. New York: Wiley; 1988. p. 399.
[6] Harris JE, Johnson RN. In: Mark HF, Bikales NM, Overberger CG, Menges G, editors. Encyclopedia of polymer science and engineering, 2nd ed, vol. 13. New York: Wiley; 1988. p. 196.
[7] Klaus CB, Susana VP, Nuns P. J Membr Sci 1993;79:83.
[8] Robison LM, Crisafulli ST. J Appl Polym Sci 1983;28:2925.
[9] Boom RM, Boomgaard TVD, Smolders CA. J Membr Sci 1994;90:231.
[10] Weber M, Heckmann W. Polym Bull 1998;40:227.
[11] Mulder M. Basic principle of membrane technology. Dordrecht: Kluwer Academic Publishers; 1996 [chapters 2–3].
[12] Callaghan TA, Paul DR. J Polym Sci, Part B 1994;32:1847.
[13] Sickafus KE, Donald AM. Br Polym J 1989;21:215.
[14] Kim JH, Kim Y, Kim CK, Lee JW, Seo SB. J Polym Sci, Part B 2003;41:1401.

[15] Kim JH, Hwang MS, Kim CK. Macromolecules 2004;37:2287.
[16] Paul DR, Barlow JW. Polymer 1984;25:487.
[17] Kambour RP, Benler TJ, Bopp RC. Macromolecules 1983;16:753.
[18] ten Brinke G, Karasz FE, Macknight WJ. Macromolecules 1983;16:1827.
[19] Zeman L, Patterson D. Macromolecules 1972;5:513.
[20] Robard A, Patterson D. Macromolecules 1977;10:1021.
[21] Kim CK, Paul DR. Polymer 1992;33:4929.
[22] Brannock GR, Paul DR. Macromolecules 1990;23:5240.
[23] Sanchez IC, Lacombe RH. J Phys Chem 1976;80:2568.
[24] Sanchez IC, Lacombe RH. J Phys Chem 1976;80:2358.
[25] Sanchez IC, Lacombe RH. Macromolecules 1978;11:1145.
[26] Sanchez IC. In: Encyclopedia of physical science and technology, vol. XI. New York: Academic Press; 1987. p. 1.
[27] Flory PJ. J Chem Phys 1942;10:51.
[28] Huggins ML. J Chem Phys 1941;9:440.
[29] Paul DR. In: Walsh DJ, Higgins JS, editors. Polymer blends and mixtures. NATO ASI series, vol. 89. Dordrecht: Martin Nijhoff Publisher; 1985. p. 1 [Series E].
[30] Sanchez IC. Polymer 1989;30:471.
[31] Flory PJ. Am Chem Soc 1965;87:1831.
[32] Eichinger BE, Flory PJ. Trans Faraday Soc 1968;64:2035.
[33] Simha R. Macromolecules 1977;10:1025.
[34] Kim JH, Barlow JW, Paul DR. J Polym Sci, Polym Phys Ed 1989;27:223.
[35] Barabas ES. In: Mark HF, Bikales NM, Overberger CG, Menges G, editors. Encyclopedia of polymer science and engineering, 2nd ed, vol. 17. New York: Wiley; 1988. p. 198.
[36] Kim MH, Kim JH, Kang YS, Park HC, Won JO. J Polym Sci, Polym Phys Ed 1999;37:2950.
[37] Kim Y, Yoo JE, Kim CK. Polymer 2003;44:5439.
[38] Palacio L, Calvo JI. J Membr Sci 1999;152:189.
[39] Fox TG. Bull Am Phys Soc 1956;1:123.
[40] Chiou JS, Paul DR. J Appl Polym Sci 1987;33:2935.
[41] Nishimoto M, Keskkula H, Paul DR. Polymer 1991;32:272.
[42] Kim CK, Paul DR. Polymer 1992;33:4941.
[43] Park DS, Kim JH, Kim CK, Lee JW. J Polym Sci, Part B 2001;39:1948.
[44] Fowler ME, Barlow WJ, Paul DR. Polymer 1986;28:1177.
[45] Alexandrocich P, Karasz FE, Macknight WJ. Polymer 1977;18:1022.
[46] Hammer CF. Macromolucules 1971;4:69.